Report of the activities on Wire Development and Wire Characterization at UNIGE in 2023

Gianmarco BOVONE[1], Florin BUTA[1], Francesco LONARDO[1], Carmine SENATORE[1,2]
[1]*Department of Quantum Matter Physics, University of Geneva, Geneva, Switzerland*
[2]*Department of Particle and Nuclear Physics, University of Geneva, Geneva, Switzerland*

Thierry BOUTBOUL, Simon C. HOPKINS
CERN, Geneva, Switzerland

This document provides an overview of key findings obtained at the University of Geneva through two collaboration agreements with CERN, operating within the framework of CHART-2. These results have been documented in scientific papers and presented at various international conferences and workshops throughout the year 2023.

The objectives of the collaborative activities with CERN are twofold:

1) To attain the targeted goal of 1500 A/mm² at 4.2 K and 16 T in a Nb_3Sn wire, demonstrating scalability for industrial-scale production over extended lengths.
2) To delineate the mechanical thresholds within which both state-of-the-art and research and development (R&D) Nb_3Sn wires can operate safely. The goal is to facilitate the development of magnets whose performance approaches the inherent limitations of the conductor.

1. Wire Development: Advanced Niobium-Tin superconductors for next generation particle colliders

Nb_3Sn is the superconducting material poised to take the place of Nb-Ti as the next step in accelerator magnet technology, but the critical current performance of state-of-the-art industrial wires is not sufficient for the development of economically and technically viable superconducting dipoles generating a magnetic field of 16 T. This target field would allow to reach a proton-proton collision energy of 100 TeV in a Future Circular Collider (FCC) with a 100-km circumference ring.

Taking as a reference the design of the Nb_3Sn wires developed for the HL-LHC upgrade, the FCC study sets a performance target of 1500 A/mm^2 for the non-Cu J_c (i.e. I_c divided by the wire area minus the Cu area), at 4.2 K and 16 T, corresponding to a layer J_c (i.e. I_c divided by the Nb_3Sn area) of 2500 A/mm^2. In Nb_3Sn the grain boundaries are the main pinning centers; therefore, materials with finer grains have higher current densities. In highly optimized rod-in-tube (RIT) wires, Nb_3Sn typically has grain sizes of ∼100–150 nm. For the dependence of pinning force on grain size reported in the literature, one can estimate that a reduction in the grain size down to 50– 60 nm would effectively enhance the non-Cu J_c beyond the FCC specification.

Internal oxidation is a practical method for inhibiting the grain growth in Nb_3Sn. This process adds an oxygen source (OS) to the wire layout and a high oxygen-affinity element to the Nb alloy. The internal oxidation of the latter forms oxide nanoparticles that lead to a reduced final Nb_3Sn mean grain size. In the previous reporting period, we documented the successful implementation of the internal oxidation process on simple multi-filamentary wires manufactured through the RIT approach. Hf or Zr

was added to the Nb alloy while SnO_2 was used as OS in two different configurations. The Nb_3Sn grain size was reduced to values below 40 nm and, regardless of the use of Hf or Zr and of the particular OS configuration, we obtained an enhancement of the layer J_c in the 2700-3000 A/mm^2 range at 16 T and 4.2 K.

In the following, we present the findings from two studies. The first study involves an experimental campaign conducted at the PHOENIX beamline of the Paul Scherrer Institute, aimed at elucidating the mechanism of oxide precipitation in internally oxidized wires. The second study explores optimal heat treatment conditions that enhance the thickness of the Nb_3Sn layer while preserving the refined grain microstructure achieved through internal oxidation.

1.1 X-Ray Absorption Spectroscopy to investigate precipitated oxides in internally oxidized Nb_3Sn wires

A comprehensive understanding of the internal oxidation process applied to the Nb_3Sn wires and, in particular, of the mechanism of oxygen transport and oxide precipitation remains elusive. To shed light on these phenomena, we employed X-ray Absorption Near Edge Structures (XANES) spectroscopy, which is particularly efficient to identify both electronic structure and chemical environment (e.g. oxidation state) of the photon absorbing atoms. The investigation was performed on multi-filamentary wires manufactured using a Nb-7.5wt%Ta-1wt%Zr starting alloy and SnO_2 as an OS. XANES spectra in fluorescence mode were gathered at the PHOENIX beamline of the Swiss Light Source at the Paul Scherrer Institute in Villigen, Switzerland. The PHOENIX beamline is specifically designed for micro-spectroscopy within the soft and tender X-ray energy ranges (0.8–8 keV) and we investigated the Zr L_3-edge, around 2223 eV. We employed the focused X-ray beam to probe the chemical environment of Zr through various regions of the wire cross-section (Nb_3Sn layer, residual alloy). Consequently, we could ascertain the fraction of Zr that precipitates as ZrO_2 and improve our understanding of how oxygen interacts with the Zr atoms present in the Nb-alloy.

We discovered that the vast majority of Zr (> 90 %) in the Nb_3Sn layer is indeed oxidized as ZrO_2, while Zr primarily remains in non-oxidized state within the residual alloy after heat treatment, akin to the Zr in the pristine alloy (not heat-treated). The presence of oxidized Zr in the Nb_3Sn layer of the samples where oxygen was initially located at the center (core) of the Nb-alloy filaments implies that oxygen can diffuse through the Nb-alloy to reach the external regions where Nb_3Sn forms, and form ZrO_2 in this layer, without oxidizing the Zr in the alloy that remains unreacted. The formation of Zr-O clusters, observed in previous works, may explain the observed modification of the XANES spectrum of the residual alloy when oxygen diffuses, but at this time we cannot be conclusive on this subject. The insights from this study serve as a valuable addition to the understanding of the internal oxidation in Nb_3Sn wires and the associated influence on superconducting properties. Future investigations are needed to determine the structure, size and distribution of the Zr-O clusters in the residual alloy, and to extend this study to hafnium in Nb_3Sn with internally oxidized Hf.

Financial support to this activity is also provided by the Swiss National Science Foundation (Grant No. 200021_184940).

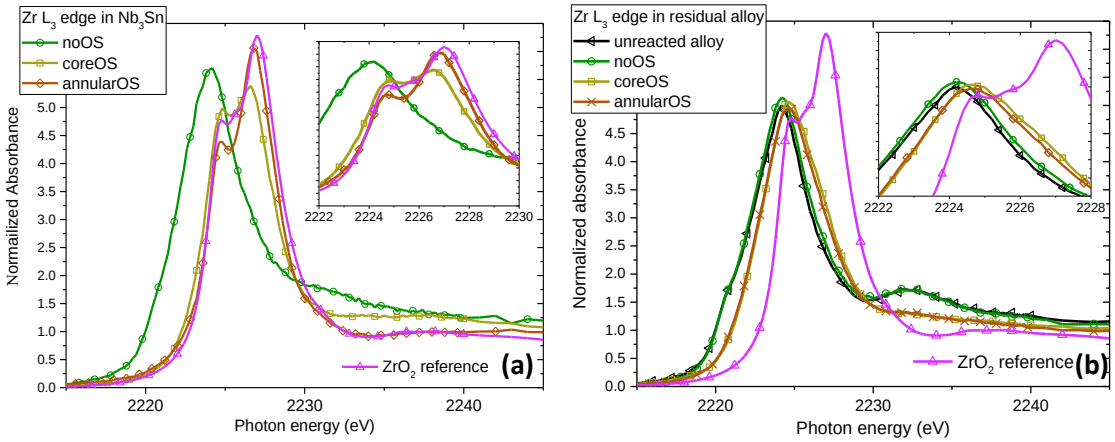

Figure 1. X-ray absorption spectra of Zr L_3 edge in Nb_3Sn of samples with and without an OS (a) and in the residual Nb alloy (b). Monoclinic ZrO_2 and unreacted Nb-alloy reference spectra are included for comparison.

1.2 Influence of the heat treatment on the layer J_c of Nb_3Sn wires with internally oxidized nanoparticles

Wires containing internally oxidized nanoparticles exhibit significantly lower Nb_3Sn layer thicknesses compared to wires based on the same Nb alloys but without an OS. By reacting wires with a Nb-alloy filament size of about 80 μm at 650°C for 200 hours, we obtained thicknesses of the Nb_3Sn fine-grained area decreasing from ~20 μm in the wires without an OS to less than 10 μm when an OS is present. Considering a typical RIT wire developed for HL-LHC, whose final Nb-alloy filament size in a subelement is approximately 1 µm and layer thickness is about 10 µm, we can argue that this important reduction of the diffusion kinetics in wires with an OS should not be a concern when implementing internal oxidation in application-ready wires. However, we decided to perform a heat treatment study for determining the effect of different heat treatment (HT) parameters, such as temperature (T) and duration of the treatment (t), on the reaction layer thickness (d_L), the final Nb_3Sn mean grain size (G_{mean}), the electrical transport properties, and the pinning mechanism of our wires. The goal of the study was to identify the reaction condition that maximize the Nb_3Sn layer thickness while retaining the refined grain microstructure produced by internal oxidation.

Heat treatment were conducted under vacuum or under Ar, in sealed quartz tubes, and were made of two distinct plateaus. The 1st plateau at 550°C for 100 hours was proposed to facilitate the diffusion of oxygen into the Nb alloy prior to the formation of Nb_3Sn. During the 2nd plateau the Nb_3Sn phase forms and grows. We systematically varied the temperature, in the 650-750°C range, and the duration, between 50 and 300 hours, of the 2nd plateau to investigate the influence of the two parameters on the reaction layer and grain size. As an example, the cross section of three wires produced with Nb-alloy filaments containing Hf and reacted at 650°C for 200 h, 700°C for 50 h and 700°C for 100°C, respectively, are compared in Figure 2. The positive effects of higher temperature and longer heat treatment duration on d_L is evident. Figure 3 reports the values of G_{mean} and of the reacted area fraction composed of fine grains, $r_{fine\ grain}$, as function of the duration for the different HT temperatures, measured on the same Hf-containing wires.

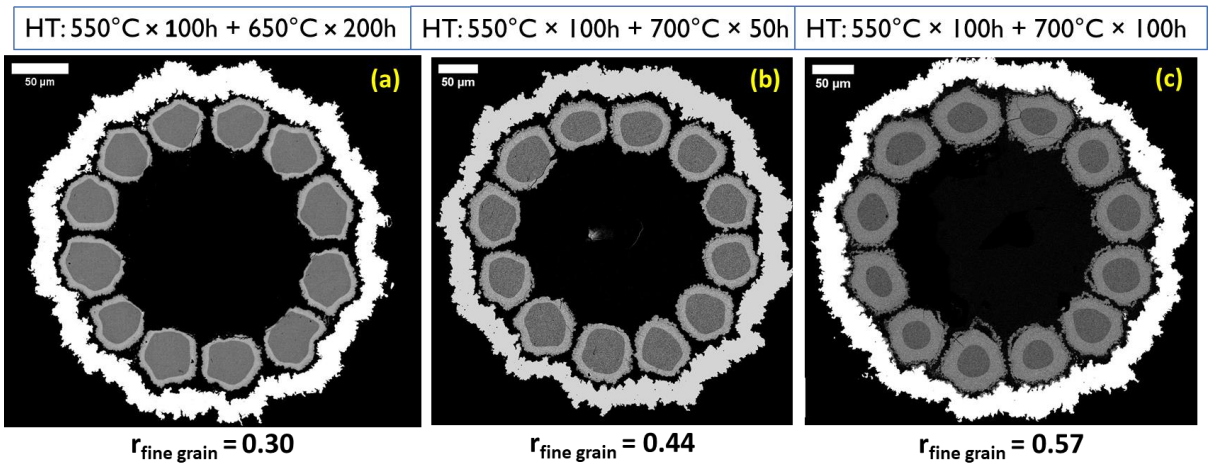

Figure 2. SEM images of the cross sections for wires based on Nb-7.5Ta-2Hf filaments and containing an oxygen source, after the 2nd plateau reaction at 650°C for 200 h (a), 700°C for 50 h (b) and 700°C for 100°C (c).

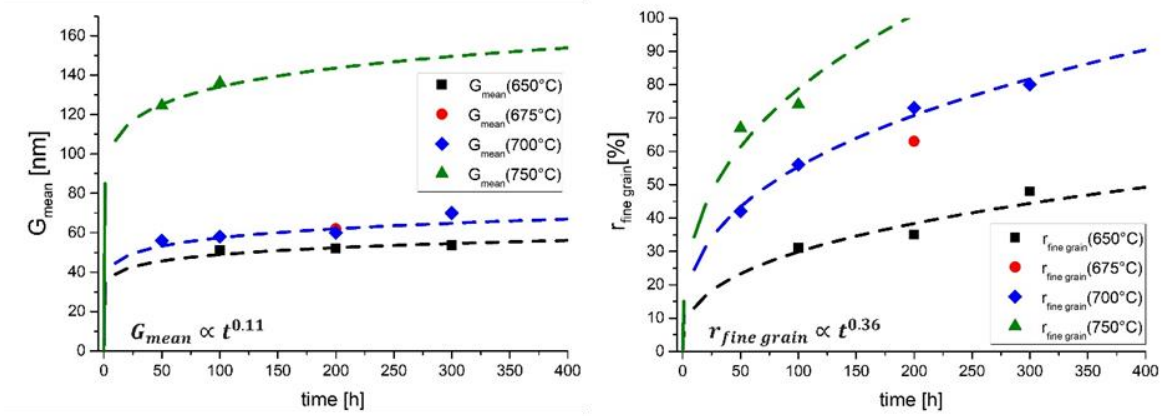

Figure 3. Values of G_{mean} (left) and $r_{fine\ grain}$ (right) for the Hf-containing wire as a function of the HT duration at various temperatures.

With the reaction at 650°C for 200 hours, the fine-grained Nb_3Sn area occupies only ~35% of the filament area for Hf-containing wires and ~20% for Zr-containing wires. After heat treatments with a reaction step at 700°C these values increase to 70-80% and ~60%, respectively, with only a minor increase of the grain size, by a maximum of 10%. Despite the limited grain growth, the layer J_c at 4.2 K and 16 T decreases from over 3000 A/mm^2 down to 1900 A/mm^2 for the Hf-containing wires, and from 2700 A/mm^2 to 1200-2200 A/mm^2 for the Zr-containing wires, as reported in Figure 4.

The decrease of the layer J_c is larger than what can be expected from the modest increase of the grain size and can be related to a change in the relative weight of pinning contributions from grain boundaries and nanoparticles. Magnetic measurements show that the high-J_c wires exhibit a point defect contribution from oxide precipitates to the pinning force, which is missing in wires with depressed J_c values. The higher heat treatment temperatures may have caused excessive coarsening of the oxide precipitates, to sizes unsuitable for flux pinning. Measurements of the size and number concentration of these nanoparticles are not available at the moment but will be performed by TEM in the near future. Further research will also explore the effects of other heat treatments between 650°C and 700°C to identify an optimal balance between retaining point defect pinning and maximizing layer growth rate.

Financial support to this activity is also provided by the Swiss National Science Foundation (Grant No. 200021_184940).

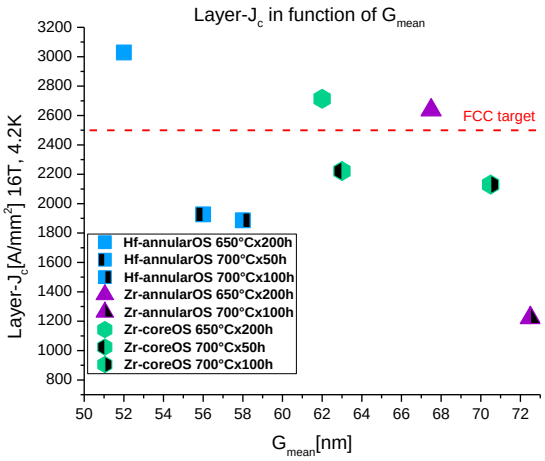

Figure 4. Values of the layer J_c at T = 4.2 K and B = 16 T as a function of G_{mean} for wires reacted following different HT schedules.

2. Wire Characterization: Multiphysical properties of advanced superconductors

Currently, a large majority of the proposed designs for the production of Nb_3Sn-based accelerator magnets in the 16 T-range entail peak stresses in the coils that are in the range of 150–200 MPa during magnet assembly and operation. These peak stresses are compressive and act in the transverse direction of the Nb_3Sn Rutherford cables used to wind the coils. As the local stresses approach and, in some cases, exceed the currently understood limits of the conductor, it becomes crucial to establish precisely the mechanical limits to be adopted in any of the magnet assembly, cooling and operation phases.

In the previous reporting period we presented a comparison of the electromechanical response to transverse compressive loads of state-of-the-art Nb_3Sn wires produced by two different technologies, restacked-rod-process (RRP®) and powder-in-tube (PIT). The experiments revealed marked differences in terms of tolerance to transverse stress between the measured RRP® and PIT wires, which follow from the different layout, composition and mechanical properties of the wire composites. The irreversible stress limit, defined as the stress level leading to a permanent reduction of the critical current by 5% at 19 T, was found to be 110 MPa for the PIT wire and in the 155–175 MPa range for the RRP® wires examined in this work.

The degradation of the critical current after unload, I_c^{unload}, can originate from the effects of the residual stresses on Nb_3Sn, which result from a plastic deformation of the Cu matrix, and from the formation of cracks. From the results of our experiments we concluded that, in spite of the different values of the irreversible stress limits, the permanent reduction of I_c^{unload} is due to the residual stress both for RRP® and PIT wires. The distortion of the Nb_3Sn lattice due to any type of stress determines a reduction of the upper critical field. This occurs when an external load acts on the superconductor as well as when the plastic deformation of the Cu matrix imposes a residual stress to Nb_3Sn. In the latter case, residual stress determines a reduction of the upper critical field after unload, $B_{c2}^{unload}(\sigma \rightarrow 0)$, with respect to the value measured on the virgin wire. The following equation proposes an expression to describe the dependence of the critical current after stress release on the magnetic field, B, and on the maximum transverse stress applied to the wire, σ :

$$I_c^{unload}\left(B,\sigma\to 0\right)=f\left(\sigma\to 0\right)C\left[\frac{B_{c2}^{unload}\left(\sigma\to 0\right)}{B}\right]^{0.5}\left[1-\frac{B}{B_{c2}^{unload}\left(\sigma\to 0\right)}\right]^{2} \quad (1)$$

with the constant prefactor C being independent of σ. $f(\sigma \to 0)$ ranges between 0 and 1 and accounts for the reduction of the current-carrying cross-section due to cracks. It follows, thus, from (1) that the percentage of critical current drop due to cracks must be constant in field. On the other hand, the field dependence of $I_c^{unload}(\sigma \to 0)$ is governed by $B_{c2}^{unload}(\sigma \to 0)$. As the residual stresses on Nb_3Sn drive the reduction of $B_{c2}^{unload}(\sigma \to 0)$, the percentage of critical current drop due to residual stresses increases with the applied field.

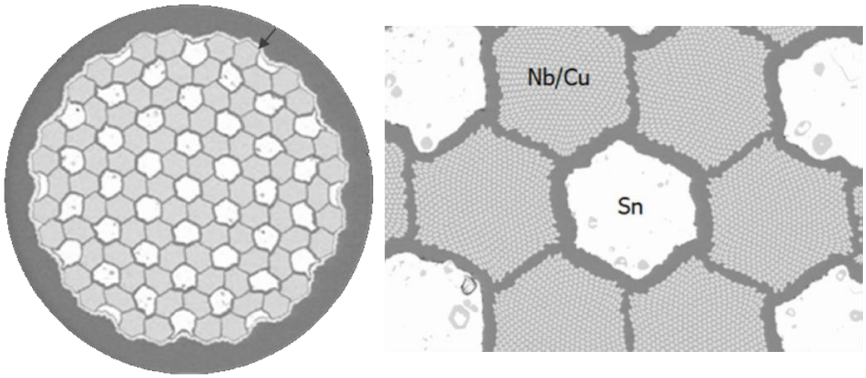

Figure 5. Cross section of the examined Distributed Tin Nb_3Sn wire examined in our experiments (left) and magnification of the filament area (right) before the reaction heat treatment.

As the dominant mechanism of degradation is controlled by the wire composite materials and architecture, which in turn are determined by the wire technology, we decided to test a high current density Nb_3Sn wire produced by a different technology, the Distributed Tin (DT) method. The fabrication of Nb_3Sn wires using the Distributed Sn method involves several sequential steps. Initially, a Nb-alloy rod is placed within an oxygen-free copper (OFC) tube and subjected to hydrostatic extrusion and cold-drawing to form filaments with a hexagonal cross-section. A large number of these Cu/Nb filaments is then restacked to form bundles. Hexagonal mono-core Sn modules are produced by cold drawing a Sn rod inserted in a OFC tube. Finally, the Nb and Sn modules are assembled within a OFC tube, with a Nb sheath serving as a diffusion barrier, and then cold-drawn to achieve the desired final wire diameter. Figure 5 shows the cross section of the DT wire used for our experiment, with a magnification of the filament area.

The examined DT wire belongs to an early development batch of JASTEC from 2014 that UNIGE received in the frame of another collaboration. After having obtained formal approval from JASTEC, it was decided to test the electromechanical properties of this wire under transverse stress. This is the first measurement of this type performed at UNIGE on Distributed Tin wires.

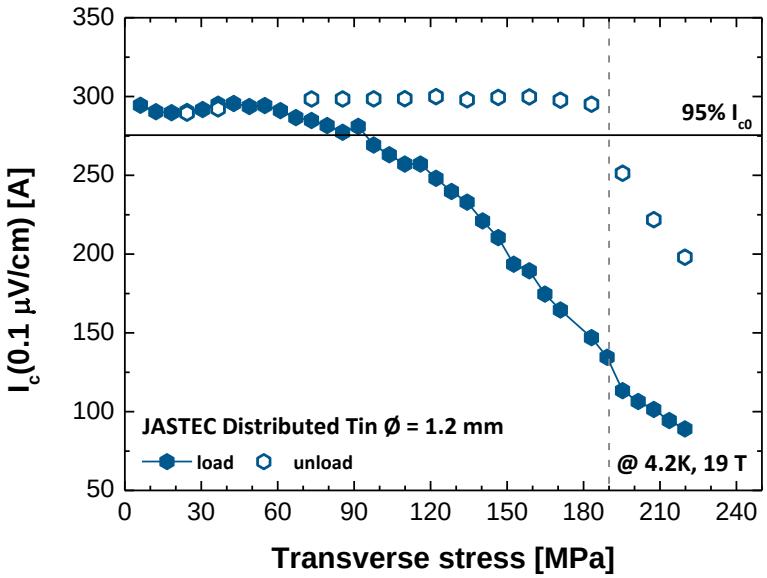

Figure 6. Dependence of the critical current I_c on the applied transverse stress for a 1.2-mm Distributed Tin wire from JASTEC impregnated with epoxy type L, at T = 4.2 K and B = 19 T. The irreversible stress limit, σ_{irr}, defined as the stress value leading to a reduction of the I_c after unload by 5% with respect to the initial I_c, is about 190 MPa.

Figure 6 shows the dependence of I_c on the applied transverse stress at T = 4.2 K and B = 19 T. Solid and open symbols correspond to the measurements under load and after unload, respectively. The force was increased in regular steps and every other step the sample was fully unloaded to monitor the irreversible reduction of I_c. All I_c values have been determined with the 0.1 µV/cm criterion over a gauge length of 126 mm. As in the case of RRP® and PIT wires, the irreversible stress limit, σ_{irr}, is defined by convention as the stress value leading to a reduction of the critical current after unload, $I_c^{unload}(\sigma \rightarrow 0)$, by 5% with respect to the critical current at zero applied stress, I_{c0}. This wire exhibits a value of σ_{irr} at 19 T of about 190 MPa. Interestingly, there is a sudden drop in the critical current values under load and after unload when the applied stress exceeds 180 MPa. Differently from what observed RRP® and PIT wires, this drop can be ascribed to the reduction of the current-carrying cross-section due to cracks: when cracks in the Nb_3Sn layer are formed, even if the critical current density of the superconductor is in principle preserved, the current-carrying cross-section and, thus, the critical current, both under load and after unload are reduced but the ratio I_c^{unload}/I_{c0} is constant in field. This experiment showcases the influence of the wire production route on the degradation mechanism under transverse compression.

3. Publications

[1] G. Bovone, F. Buta, F. Lonardo, M. Bonura, C. N. Borca, T. Huthwelker, S.C. Hopkins, A. Ballarino, T. Boutboul and C. Senatore, " X-Ray Absorption Spectroscopy to investigate precipitated oxides in Nb_3Sn wires with an internal oxygen source," IEEE transactions on Applied Superconductivity **34** 3, 6000205 (2024) https://doi.org/10.1109/TASC.2024.3354232

[2] F. Lonardo, G. Bovone, F. Buta, M. Bonura, T. Bagni, B. Medina-Clavijo, A. Ballarino, S. C. Hopkins, T. Boutboul and C. Senatore " Influence of the heat treatment on the layer J_c of internal-Sn Nb_3Sn wires with internally oxidized nanoparticles," IEEE Transactions on Applied Superconductivity **34** 5, 6000305 (2024) https://doi.org/10.1109/TASC.2024.3355353

[3] G. Bovone, F. Buta, F. Lonardo, T. Bagni, M. Bonura, D. LeBoeuf, S.C. Hopkins, T. Boutboul, A. Ballarino and C. Senatore, " Effects of the oxygen source configuration on the superconducting properties of internally-oxidized internal-Sn Nb_3Sn wires," Superconductor Science and Technology **36** 9, 095018 (2023). https://doi.org/10.1088/1361-6668/aced25

[4] T. Bagni, G. Bovone, A. Rack, D. Mauro, C. Barth, D. Matera, F. Buta, C. Senatore, " Degradation of I_c due to residual stress in high-performance Nb_3Sn wires submitted to compressive transverse force," Superconductor Science and Technology **36** 7, 075001 (2023) https://doi.org/10.1088/1361-6668/acca50

4. Presentations at conferences and workshops

- *Current Trends and Future Prospects for the High-Field Applications of Nb_3Sn and REBCO Superconductors*
  Presenting author: Carmine SENATORE, invited oral at the Summit of Material Science 2023 and GIMRT User Meeting 2023, Sendai, Japan, November 20 – 22, 2023;
- *Nb_3Sn wire development by Internal Oxidation at UNIGE*
  Presenting author: Gianmarco BOVONE, invited oral at CERN High Field Magnet Annual Meeting 2023, Geneva, Switzerland, October 30 – November 2, 2023;
- *Investigating the impact of transverse compressive stress on Nb_3Sn wires for high-field accelerator magnets*
  Presenting author: Carmine SENATORE, contributed oral at 28th International Magnet Technology Conference, MT-28, Aix-en-Provence, France, September 10 – 15, 2023;
- *Influence of the heat treatment on the layer-J_c of internal-Sn Nb_3Sn wires with internally oxide nanoparticles*
  Presenting author: Francesco LONARDO, contributed oral at 28th International Magnet Technology Conference, MT-28, Aix-en-Provence, France, September 10 – 15, 2023;
- *X-Ray Absorption Spectroscopy to investigate precipitated oxides in Nb_3Sn wires*
  Presenting author: Gianmarco BOVONE, contributed oral at EUCAS2023, the 16th European Conference on Applied Superconductivity, Bologna, Italy, September 3 – 7, 2023;